AD-A088 050 NAVAL RESEARCH LAB WASHINGTON DC F/G 4/2
NUMERICAL SIMULATION OF THE INFLUENCE OF SEA-SURFACE TEMPERATUR--ETC(U)
JUL 80 S W CHANG, R V MADALA
UNCLASSIFIED NRL-MR-4272 NL

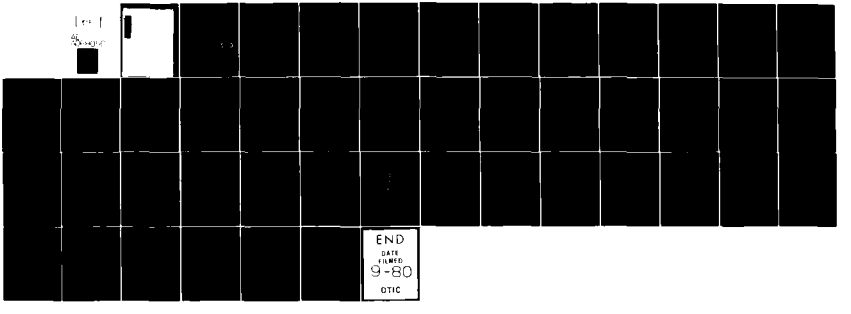

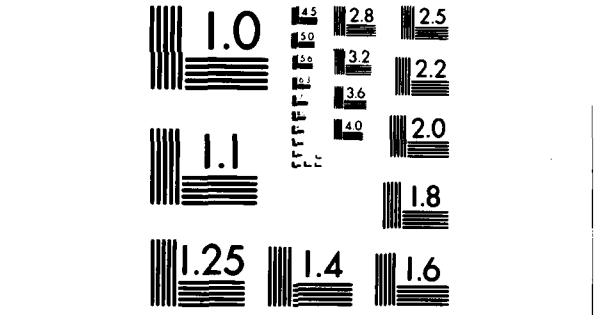

SECURITY CLASSIFICATION OF THIS PAGE (When Data Entered)

REPORT DOCUMENTATION PAGE

READ INSTRUCTIONS BEFORE COMPLETING FORM

1. REPORT NUMBER: NRL Memorandum Report 4272	2. GOVT ACCESSION NO.: AD-A088 050
3. RECIPIENT'S CATALOG NUMBER	
4. TITLE (and Subtitle): NUMERICAL SIMULATION OF THE INFLUENCE OF SEA-SURFACE TEMPERATURE ON TRANSLATING TROPICAL CYCLONES	5. TYPE OF REPORT & PERIOD COVERED: Interim report on a continuing NRL problem.
	6. PERFORMING ORG. REPORT NUMBER
7. AUTHOR(s): Simon W. Chang and Rangarao V. Madala	8. CONTRACT OR GRANT NUMBER(s): 17 Jul 80
9. PERFORMING ORGANIZATION NAME AND ADDRESS: Naval Research Laboratory, Washington, D.C. 20375 (14) NRL-MR-4272	10. PROGRAM ELEMENT, PROJECT, TASK AREA & WORK UNIT NUMBERS: 62759N; 9F52-551-792; 9F52-551-792; 67-0909-0-0
11. CONTROLLING OFFICE NAME AND ADDRESS: Naval Air Systems Command, Washington, D.C. 20361	12. REPORT DATE: July 17, 1980
	13. NUMBER OF PAGES: 46
14. MONITORING AGENCY NAME & ADDRESS (if different from Controlling Office): (16) F51.551 (17) 9F52551792	15. SECURITY CLASS. (of this report): UNCLASSIFIED
	15a. DECLASSIFICATION/DOWNGRADING SCHEDULE

16. DISTRIBUTION STATEMENT (of this Report)

Approved for public release; distribution unlimited.

DTIC ELECTE AUG 20 1980 S D B

17. DISTRIBUTION STATEMENT (of the abstract entered in Block 20, if different from Report)

18. SUPPLEMENTARY NOTES

*Present address: JAYCOR, 205 Whiting Street, Alexandria, VA 22304.

This research was partially supported by the Office of Naval Research.

19. KEY WORDS (Continue on reverse side if necessary and identify by block number)

Tropical cyclones
Sea-surface temperature
Air-sea interaction

20. ABSTRACT (Continue on reverse side if necessary and identify by block number)

A three-dimensional numerical model with a domain of 3000 X 3000 km is used to study the influence of sea-surface temperature (SST) on the behavior of tropical cyclones translating with mean flows in the Northern Hemisphere.

We find that tropical cyclones tend to move into regions of warmer SST when a gradient of SST is perpendicular to the mean ambient flow vector (MAFV). The model results also indicated that a region of warmer SST situated to the right side of the MAFV is more favorable for storm intensification than to the left side due to the asymmetries in air-sea energy exchanges associated

(Continues)

20. Abstract (Continued)

with translating tropical cyclones. The model tropical cyclone intensifies and has greater rightward deflection in its path relative to the MAFV when translating into the region of warmer SST. The model tropical cyclone intensifies when its center travels along a warm strip, it weakens along, but does not move away from a cool strip.

The results suggest that the SST distribution not only affects the intensity and path of tropical cyclones frictionally, but also affects them thermally through processes of heating redistribution and geostrophic adjustment.

CONTENTS

I.	Introduction	1
II.	The Numerical Model	3
III.	The Control Experiment	6
IV.	Tropical Cyclone Translating into Broad Regions of Warm and Cool SST	7
V.	Tropical Cyclone Translating Perpendicular to SST Gradient	10
VI.	Tropical Cyclone Translating into Strips of Warm or Cool SST	13
VII.	Summary	14
	Acknowledgments	17
	References	18
	Figures	22

NUMERICAL SIMULATION OF THE INFLUENCE OF SEA-SURFACE TEMPERATURE ON TRANSLATING TROPICAL CYCLONES

I. INTRODUCTION

Unlike their counterparts in mid- and higher-latitudes where the contrast of air masses provides enough energy for circulation, tropical cyclones depend on the ocean for their energy source. Sensible and latent heat transported through the air-sea interface, in cooperation with the frictionally-induced inflow, supplies the energy for maintaining the tropical cyclone circulation. The air-sea interaction is an important physical process that affects the behavior of tropical cyclones.

Observational studies on the interaction of tropical cyclones and the ocean have indicated a strong dependence of tropical cyclones on the sea-surface temperature (SST). The development, intensification, and movement of tropical cyclones are in many instances linked with the warm SST (Palmen, 1948; Fisher, 1958; Miller, 1958; Perlroth, 1967; Brand, 1971; Gray, 1979). Because the ocean is regarded as the heat reservoir, attention has also been focussed on the importance of the thermal structure of the upper ocean. It is found that warm and deep oceanic mixed layers are necessary conditions for the development and intensification of tropical cyclones (Tisdale and Clapp, 1963; Perlroth, 1969). Contrary to the above findings, some tropical cyclones are not affected by SST (Ramage, 1972; 1974).

Earlier numerical studies with axisymmetrical (therefore stationary) models showed that tropical cyclones are very sensitive to small changes of SST (Ooyama, 1969; Rosenthal, 1971; Sundquist, 1972). Typically, a 50% change in model maximum wind would result from a $2^{o}C$ change of SST. By incorporating a better parameterization of the atmospheric boundary layer (ABL), Anthes and Chang (1978) showed that an axisymmetric tropical cyclone is not as sensitive as earlier studies indicated. The enhanced (decreased)evaporation associated

Manuscript submitted May 29, 1980.

with warm (cool) SST is partially compensated for by the increased (decreased) surface friction, therefore, the tropical cyclone has a 12h delay in response to SST changes. When their tropical cyclone was coupled with the ocean, the response was even weaker and further delayed (Chang and Anthes, 1979). However, the long term behavior of their model cyclone still agreed with previous axisymmetric model studies, i.e., warmer SST results in intensification and cooler SST results in weakening.

The motion of a tropical cyclone with mean flow over an ocean of uniform SST has been studied by Kuo (1969) and Jones (1977a) using linear models. The air-sea interactions in these two linear models were purely mechanical with only surface friction. These studies indicated that the trajectory of the vortex center is a damped trochoid. The deflection angle of the mean path (the angle between the mean current and the mean vortex motion) is a function of the surface friction and the environmental friction. For tropical cyclones, where the surface friction is greater than the environmental friction, the deflection is usually to the right of the mean flow. These results were later substantiated by Jones' (1977) three-dimensional, non-linear model with uniform SST.

The behavior of tropical cyclone in a three-dimensional model with mean flow over non-uniform SST has not been studied. With variations in SST, both the intensity and movement of tropical cyclones may be more complex. The surface friction will change because of variations in surface stability associated with the non-uniform SST, the sensible and latent heat exchanges may be in certain ways dictated by the SST distributions. These variations may significantly affect the behavior of tropical cyclones.

The purpose of this study is to investigate the influence of various non-uniform SST distributions on the intensities and movements of tropical cyclones that are imbedded in a mean flow. As described in the next section, the model domain is large enough to allow free movement of the tropical cyclone for about 3-4 days. The parameterization of the ABL has been improved so that the air-sea interaction is adequately treated. In Section III, the life history of a weak tropical cyclone translating over ocean with uniform SST will be discussed and used as the control experiment for later comparison. In Section IV, we first examine the responses of tropical cyclones when translating into regions of warmer and cooler SST. In Section V, the response of the translating tropical cyclone with SST gradients perpendicular to the mean flow will be discussed. Finally, the repsonse of the translating tropical cyclone encountering strips of warmer or cooler SST will be discussed in Section VI.

II. THE NUMERICAL MODEL

The tropical cyclone model used is identical to the one described in Madala and Chang (1979).[1] The governing equations include the primitive equations of conservation for horizontal momentum, mass, enthalpy, and water vapor. The system of equations is hydrostatic. A normalized pressure (σ) is the vertical coordinate (Phillips, 1957). The physics includes the subgrid scale horizontal mixing, the subgrid scale cumulus convection, the grid scale precipitation, and the subgrid scale vertical mixing due to surface friction.

The subgrid scale horizontal mixing is parameterized by a kinematic eddy coefficient. This coefficient consists of a constant part and a part linearly

dependent on wind speed. This form of the eddy coefficient yields suitable mixing in the initial as well as the mature stages (Anthes et al. 1971).

The subgrid scale cumulus convection is parameterized following Kuo's (1974) and Anthes's (1977) methods. Conditional instability and the boundary layer convergence of water vapor are prerequisites for the cumulus convection. The partitioning of heating and moistening depends on the vertically averaged relative humidity of the air column. The vertical distribution of heating is determined by the amount of conditional instability and the prescribed weighting functions (see Anthes and Chang, 1979). The use of the weighting functions insures a proper vertical heating distribution for the growth of tropical cyclone scale disturbances. The grid scale precipitation occurs when the air reaches saturation in grid scale lifting.

The boundary layer effects are parameterized based on a generalized similarity theory in which the logarithmic-linear profiles of the momentum, temperature, and water vapor are "match" into the mixed layer (Chang and Madala, 1980).[2] Anthes and Chang (1979) have shown a higher resolution BL is superior to a single layer bulk ABL in an axisymmetric tropical cyclone model. To incorporate into a 3D tropical cyclone model a higher resolution ABL is economically prohibitive. In addition, the results of Anthes and Chang (1979) indicate that, except for the period of rapidly changing stability, the ABL in tropical cyclones is dominated by mechanical mixing. Therefore, matching technique seems to be appropriate. Universal functions A, B, C, and D are formulated following Yamada (1976). The surface roughness height over open water are calculated by Chanock's equation (Delsol et al, 1970).

The model atmosphere from P = Ps (surface) to P = 0 is divided into seven sigma layers (Figure 1). Note that the lowest layer has a thickness of about 700 m, which is the typical ABL depth in tropical cyclones (Moss and Merceret, 1976; Anthes and Chang, 1979). A better vertical resolution between $\sigma = 0.1$ and $\sigma = 0.3$ is used to resolve the tropopause and outflow structure. All prognostic variables such as u, v, T, and q, are defined at the center of each layer, all diagnostic variables such as $\dot{\sigma}$ and ω are defined at the boundary of each layer. The momentum points and mass points are fully staggered in horizontal direction following Arakawa scheme C. The spatial differencing is second order to conserve mass, momentum, and enthalpy.

The tropical atmosphere of the hurricane season (Sheets, 1971) is used for the initial mean thermodynamic state of the model. The thermal structure features a conditionally unstable lapse rate from surface to about 350 mb and high relative humidity (RH) up to 500 mb.

The initial flow field includes a uniform easterly current of about 4.5 m s^{-1} and a non-divergent, idealized vortex with maximum wind of 16 m s^{-1}. The initial surface pressure and temperature field are in gradient balance with the flow field. The Coriolis parameter is 5×10^{-5} s^{-1}. One effect of latitudinal variation of Coriolis parameter is to produce a northward movement of the vortex (Madala and Piacsek, 1975; Anthes and Hoke, 1975). For the purpose of isolating the movement of tropical cyclones caused by SST, the Coriolis parameter is set constant in this study.

III. THE CONTROL EXPERIMENT

A tropical cyclone with rather weak intensity develops from the initial vortex imbedded in the uniform easterly mean flow of approximately 4.5 m s^{-1} over an ocean of 28.5 C. The model tropical cyclone reaches a quasi-steady state after 48 h, attaining a minimum pressure of 996 mb^{-1} and maximum ABL wind speed in the lowest layer of the model of 32 m s^{-1} (this experiment is referred to as the control experiment (Exp. A, see Table 1)).

Figure 2 shows the ABL flow pattern and the surface pressure field at 84 h when the model integration was terminated. The strong circulation is confined to the region near the storm center. Maximum winds are located to the right of the storm track where the cyclonic circulation and the mean current is in the same direction. The winds at the center are very weak. The flow far from the storm circulation is nearly undisturbed by the storm. These characteristics of the low-level flow are also implied by the surface pressure field. The circular isobars and the stronger pressure gradient are concentrated to the region near the storm center.

Contrary to the concentrated cyclonic circulation at low level, the asymmetric flow at the outflow level (σ = 0.1 - 0.2) is predominantly anti-cyclonic with a small region of cyclonic circulation near the center. The speed of the anticyclonic circulation increases away from the center in conservation of the angular momentum. It reaches a maximum of more than 20 m s^{-1} to the southeast* of the storm center.

*Because the Coriolis parameter is constant, the orientation of the domain has no real geophysical meaning.

As shown by the paths of the storm center, the storm moves downstream with the mean current and with a deflection to the right of the MAFV. At 84 h, the net northward displacement of the storm center is about 100 km. The 5^{o} deflection angle of our model is very typical for model tropical cyclones (Jones, 1977a). However, the small scale looping motion in the trochoid (Jones, 1977b) cannot be resolved by the 60 km grid resolution of the present model.

Figure 3 shows the stress field at 84 h of Exp. A. Comparing with the surface wind field, the region of the strongest stress is located to the right of the storm track. The crescent shape of the maximum stress region is responsible for the often observed crescent-shaped maximum cooling in the ocean (Black, 1972). To the south of the strong stress, there is a region where the stress is very small, corresponding to the weak surface wind at the storm center.

The evaporation rate at 84 h of Exp. A shows that the strongest evaporation occurs outside and to the north of the region of the maximum wind (Fig. 4) where the ABL winds are considerable and the humidity is undersaturated. The maximum evaporation rate is approximately 2.5 cm day^{-1}. The sensible heating is relatively insignificant, in agreement with earlier findings of Rosenthal (1971) and Anthes and Chang (1978).

A series of experiments with various non-uniform SST distributions were performed. The schematical patterns of SST tested are shown in Figures 5 and listed in Table 1.

IV. TROPICAL CYCLONES TRANSLATING INTO BROAD REGIONS OF WARM AND COOL SST

As mentioned before, the intensity of axisymmetric, stationary model tropical cyclones is sensitive to sudden changes of SST. The situation that

Table 1. SUMMARY OF EXPERIMENTS AND RESULTS

Experiment	SST Patterns	Path	Final Max. Wind ($m\ s^{-1}$)
A	Uniform SST, 28.5 C	$\sim 5^{o}$ to the right of MAFV	33
W	Broad region of 2 C warmer SST	$\sim 7^{o}$ to the right of MAFV	50
C	Broad region of 2 C cooler SST	$\sim 3^{o}$ to the right of MAFV	22
WR	Warmer SST to the right with gradient perpendicular to MAFV	Moves toward warm SST deflection angle 17^{o}	50
WL	Warmer SST to the left with gradient perpendicular to MAFV	Moves toward warm SST deflection angle $\sim -5^{o}$	31
WS	2 C warm strip parallel to MAFV	Same as Control	50
CS	2 C cool strip parallel to MAFV	Same as Control	25
WS45	2 C warm strip at 45^{o} angle to MAFV	Same as Control	34

we consider here is a tropical cyclone that translates into regions of warmer or cooler SST. The response of the tropical cyclone in this more realistic situation is investigated with Exp. W., where the SST is 2 C warmer at 30.5 C in the western half of the domain, and Exp. C, where the SST is 2 C cooler at 26.5 C in the western half of the domain. SST in the eastern half of the domain stays at 28.5 C.

Figure 6 shows the time series of the minimum pressures of Exps. W and C and the control (Exp. A). In both Exps. W and C, the minimum pressures deviate very little from the control experiment until the center of the storm moves into the region of warmer or cooler SST. The delay is also evident in the maximum surface wind (Figure 7). This delayed response, similar to the behavior of the axisymmetric model of Anthes and Chang (1978), is due to the increased (decreased) dissipation of kinetic energy which partially compensates for the enhanced (weakened) evaporation over the warm (cool) SST.

The SST patterns tested here also affect the path of the tropical cyclone. At 84 h, the storm centers in Exps. W and C are displaced to about 60-100 km to the right and left, respectively, relative to the control experiment (Figure 8). The fact that the increased surface friction produces a stronger deflection to the right of the MAFV agrees qualitatively with the linear theories of Kuo's (1969) and Jones' (1977a). But in contrast to the linear theory, the variation in the surface friction may be due to both storm intensity and the surface stability. As it becomes clearer in the experiments discussed in the next section, the asymmetries associated with a translating tropical cycline and air-sea thermal exchange can also contribute to the deflection. Most of the air-sea exchanges of sensible and latent heats occur in the right half of

the tropical cyclone relative to the MAFV, and have important thermal effects on the paths of tropical cyclones other than the mechanical effects considered previously. As shown in Figure 9, stronger evaporation mainly occurs over the region of warmer SST at 27 h of Exp. W. The maximum evaporation rate increases from about 2 cm day^{-1} at 24 h to more than 6 cm day^{-1} at 36 h in Exp. W when the center of the storm moves into the region of warmer SST. Such a strong and asymmetric evaporation distribution causes a stronger convection and heating to the right of the MAFV and shifts the storm center toward the north.

V. TROPICAL CYCLONE TRANSLATING PERPENDICULAR TO SST GRADIENT

To further differentiate ocean's thermal effect on the path of tropical cyclones, we now consider the case that the mean flow is perpendicular to SST gradient. In Exp. WR, the SST is 30.5 C to the right and 26.5 C to the left of the MAFV, and in between the 30.5 C and 26.5 C waters, there is a 600-km wide region where the SST increases continuously toward the right having a gradient of 4 C/600 km. In Exp. WL, the SST pattern is reversed so that the warm and cool ocean waters are located to the left and right of the MAFV, respectively, and the SST gradient is toward the left in the central region.

These SST patterns have very noticeable influence on both the intensity and the path of the model tropical cyclone. As illustrated in Figs. 10 and 11, the storm intensity of Exp. WR increases greatly to a central pressure of 982 mb and maximum wind of 50 m s^{-1} at 84 h; whereas the storm intensity in Exp. WL remains essentially unchanged. The storm centers

in both Exps. WR and WL are displaced perpendicular to the MAFV from the control experiment by more than 200 km toward the regions of warmer SST (Fig. 12). At 84 h, the center of circulation in Exp. WR has almost entered the region of 30.5C water. The apparent tendency of the model tropical cyclone to move toward the warm SST is caused by the enhanced latent heating associated with the SST distributions.

As illustrated by the evaporation rate at 27 h (Figures 13 and 14), the evaporation in Exp. WR occurs mainly over the warm water to the right of the MAFV while the evaporation in Exp. WL occurs mainly to the left of the MAFV. Both the rate of evaporation and the area of strong evaporation in Exp. WR is much larger than in Exp. WL. Due to the asymmetry associated with the translating tropical cyclone, the surface wind and the surface stress are stronger to the right of the MAFV (see Figure 2 and 3). In Exp. WR the region of stronger stress coincides with the region of warmer SST, whereas in Exp. WL, the region of stronger stress does not coincide with the region of warmer SST. Consequently, the maximum evaporation rate increases to $6 \sim 7$ cm d^{-1} in Exp. WR, it remains at about 2 cm d^{-1} in Exp. WL. The stronger evaporation in Exp. WR causes the intensification.

Increased evaporation and enhanced surface friction also cause a local increase in the total energy convergence over the region of the warmer SST. The temperature of the air column above the region of the warmer SST will then increase through cumulus heating and the surface

pressure will ultimately fall. A gradual shift of the low pressure center toward the warmer SST, through geostrophic adjustment, results in a displacement of the vortex. This gradual shift makes the storm centers in both experiments move toward the warm SST perpendicular to the MAFV.

Note also that the rightward deflection from the control path in Exp. WR is larger than that in Exp. W, and the leftward deflection from the control path in Exp. WL is larger than that in Exp. C, where the storm intensity is weaker than Exp. WL. This behavior cannot be explained by the linear theories where the hurricane-ocean interaction is merely mechanical. The SST distribution causes a redistribution of the latent heating, and through geostrophic adjustment, shifts the circulation center toward the warm water.

Several investigators have used the total thermal potential as a measure of the energy available for the development of incipient tropical cyclones (Perlroth, 1969; Leipper and Volgenan, 1972). As illustrated by Exps. WR and WL, the storm intensities and paths are very different in spite of the fact that the total oceanic thermal potentials in two cases are identical. This confirms the finding in Chang (1979) that the air-sea energy exchange in the tropical cyclone and ocean system depends very much on the details of the relative location, size, and magnitude in SST variations.

VI. TROPICAL CYCLONE TRANSLATING INTO STRIPS OF WARM OR COOL SST

We now examine the response of the tropical cyclone when it passes over strips of warmer or cooler SSTs. As depicted in Figure 5, the SST patterns include (1) a 300-km-wide 2C warm strip parallel to the MAFV (Exp. WS), (2) a 300-km-wide 2C cold tongue parallel to the MAFV (Exp. CS), and (3) a 300-km-wide 2C warm strip at 45^{o} angle to the right of the MAFV.

The response of the model tropical cyclone to the warm or cold strip is not noticeable until after 36 h when the center of the storm moves into the warm or cold tongue. At 84 h, the minimum pressures of Exps. WS and CS are respectively 980 and 1000 mb, and the maximum surface winds are respectively 50 and 25 m s^{-1} (Figures 15 and 16).

Contrary to the finding that tropical cyclones tend to steer away from a pool of cold ocean water, the paths of the storm centers in Exps. WS and CS are essentially unchanged as compared to the control Exp. A despite the difference in storm intensity (Figure 13). It is probably due to the fact that the changes in surface friction are restricted to the relatively small regions of warm or cold strips.

The model tropical cyclone has very little response to the warm strip which lies at 45^{o} angle to the MAFV (Exp. WS45). Previous experiments with axisymmetric hurricane model (Anthes and Chang, 1978; Chang and Anthes, 1979) showed that a tropical cyclone does not respond to warm SST if the

tropical cyclone overlays the region of warmer SST for less than 12 h. The storm in Exp. WS45 travels through the region of warmer SST in less than 15 h, which is apparently not long enough for the tropical cyclone to have significant response before it leaves the warm strip.

The variation in SST affects the air-sea exchange of sensible and latent heat. As shown by Figure 14, the strong evaporation at 30 h of Exp. WS occurs mainly in the region of the warm SST. The strongest evaporation occurs near the leading (northern) edge of the warm tongue. The evaporation in Exp. CS is much weaker over the cold tongue except for a slight increase where the air flow re-enters the region of 28.5C water. Changes in the evaporation near the storm center, over a period of time, results in changes in the intensities of the tropical cyclone. There are many other fine details in the momentum field of the tropical cyclone induced by the warm and cold strips. For example, before the center of the tropical cyclone and the major portion of the strong cyclonic circulation enter the region of change SST, the low-level flow reacts to the warm strip in a fashion similar to that of a heat island. Upward motion is induced in the ABL due to temperature gradient within the edge of the warm ocean. These changes in the momentum field are persistent, but localized, and do not seem to affect the overall behavior of the tropical cyclone.

VII. SUMMARY

The influence of various SST distributions on the intensities and paths of translating tropical cyclones has been investigated using a three dimensional model of tropical cyclones with improved parameterization of the ABL and Kuo's (1974) cumulus parameterization.

Various distribution of the SST are tested and found to have considerable influence on the intensity and path of the model tropical cyclone (see Table 1). The variations in the SST not only changes the total surface friction, which controls the deflection of the vortex from the mean ambient flow, but also alters the sensible and latent heat exchanges. The magnitude and the spatial distribution of the heat exchanges affect the intensity as well as the movement of the tropical cyclone. Major results are summarized as follows:

1. There is a deflection of approximately five degrees to the right of MAFV as a slowly varying tropical cyclone translates on an f-plane with mean flow over an ocean of uniform SST.

2. The intensity and the angle of deflection increases with increased SST due to enhanced evaporation and friction.

3. When translating downwind the mean flow over the ocean with SST gradients perpendicular to the MAFV, tropical cyclones tend to move into the region of warmer SST. The movement toward warm SST is gradual and continouous.

4. Tropical cyclones are more likely to intensify when warmer ocean situates to the right (left) of the storm track than to the left (right) in the Northern (Southern) Hemisphere because of the asymmetries associated with translating tropical cyclones.

5. Narrow (as compared to the storm size) regions of warmer or cooler SST have little influence on the paths of tropical cyclones. However, if the central portion of the tropical cyclone overlays the narrow region of warm (cooler) SST over a period of time (> 12 h), the tropical cyclone intensifies (weakens).

From these results, we conclude that the SST distribution affects the behavior of a translating tropical cyclone, both frictionally and thermally. In agreement with the adiabatic linear theories, the translating tropical cyclone appears to deflect more to the right of the mean flow when friction is increased (either due to increased surface instability or stronger intensity). The SST distribution also redistributes the available latent energy. This causes a shift in heating and pressure tendency, and ultimately a shift of the vortex by geostrophic adjustment, toward the warm ocean.

In light of these results, an increased effort to obtain and utilize accurate SST data in operational forecast of tropical cyclones deserves more serious consideration.

ACKNOWLEDGEMENTS

The research is supported by the Naval Environmental Prediction Research Facility Block Fund and the Naval Research Laboratory Contract N00173-78-C-426. We thank Drs. Winston C. Chao, Mark R. Schoeberl, and Darrell F. Strobel for comments on the manuscript, and Mrs. Jane Polson for typing the manuscript.

REFERENCES

Anthes, R. A., 1972: Development of asymmetries in a three-dimensional numerical model of the tropical cyclone. Mon. Wea. Rev., 100, 461-476.

Anthes, R. A. 1977: A cumulus parameterization scheme utilizing a one-dimensional cloud model. Mon. Wea. Rev., 105, 270-286.

Anthes, R. A., and S. W. Chang, 1978: Response of the hurricane boundary layer to changes of sea surface temperature in a numerical model. J. Atmos. Sci., 35, 1240-1255.

Anthes, R. A., and J. E. Hoke, 1975: The effect of horizontal divergence and the latitudinal variation of the Coriolis parameter on the drift of a model hurricane. Mon. Wea. Rev., 103, 757-763.

Anthes, R. A., S. L. Rosenthal, and J. W. Trout, 1971: Preliminary results from an asymmetric model of the tropical cyclone. Mon. Wea. Rev., 99, 744-758.

Black, P. G., 1972: Some Observations from Hurricane Reconnaissance Aircraft of Sea-Surface Cooling Produced by Hurricane Ginger (1971). Mariner's Weather Log, 64, 288-298.

Brand, S., 1971: The effects of tropical cyclone of cooler surface waters due to upwelling and mixing produced by a prior tropical cyclone. J. Appl. Meteor. 10, 865-874.

Chang, S. W., 1979: The response of an axisymmetric model tropical cyclone to local variations of sea surface temperature. Mon. Wea. Rev., 107, 662-666.

Chang, S. W. and R. A. Anthes, 1979: The mutual response of the tropical cyclone and the ocean. J. Phys. Oceanogr., 9, 128-135.

Chang, S. W. and R. V. Madala, 1979: Planetary boundary layer parameterization for tropical cyclones based on Generalized Similarity Theory, Naval Research Laboratory, Technical Report.

Delsol, F. K. Miyakoda, and R. H. Clarke, 1970: Parameterized processes in the surface boundary layer of an atmospheric circulation model. Quart. J. Roy. Meteor. Soc., 97, 181-208.

Fisher, E. L., 1958: Hurricane and the sea-surface temperature field. J. Meteor., 15, 328-333.

Gray, W. M., 1979: Hurricanes: their formation, structure, and likely role in the tropical circulation. Quart. J. Roy. Soc. Meteor., 155-217.

Jones, R. W. 1977a: Vortex motion in a tropical cyclone model. J. Atmos. Sci., 32, 1518-1527.

Jones, R. W., 1977b: A nested grid for a three-dimensional model of a tropical cyclone. J. Atmos. Sci., 34, 1538-1553.

Kuo, H. L., 1969: Motions of vortices and circulating cylinder in shear flow with friction. J. Atmos. Sci., 26, 390-398.

Kuo, H. L., 1974: Further studies of the parameterization of the influence of cumulus convection on large scale flow. J. Atmos. Sci., 31, 1232-1240.

Leipper, D. F., and D. Volgenau, 1972; Hurricane Heat Potential of Gulf of Mexico, J. Phys. Oceangr., 2, 218-224.

Madala, R. V. and S. W. Chang, 1979: A vectorized three-dimensional operational tropical cyclone model. Preprint Scientific Computer Information Exchange Conference, August 1979, Livermore.

Madala, R. V. and S. A. Piacsek, 1975: Numerical simulation of asymmetric hurricane on a β-plane with vertical shear. Tellus, 27, 453-468.

Miller, B. I., 1958: On the maximum intensity of hurricanes, J. Meteor., 15, 184-195.

Moss, M. S., and F. J. Merceret, 1976: A note on several low-layer features of hurricane Eloise (1975). Mon. Wea. Rev., 104, 967-971.

Ooyama, K., 1969: Numerical simulation of the life cycle of tropical cyclones. J. Atmos. Sci., 26, 3-40.

Palmen, E., 1948: On the formation and structure of tropical hurricanes, Geophysics, 3, 26-38.

Perlroth, I., 1967: Hurricane behavior as related to oceanographic environmental conditions. Tellus, 19, 258-267.

_____ 1969: Effects of oceanographic media on equatorial Atlantic hurricanes. Tellus, 21, 230-240.

Ramage, C. S., 1972: Interaction between tropical cyclones and the China Sea. Weather, 27, 484-494.

Ramage, C. S., 1974: The typhoons of October 1970 in the South China Seas: Intensification, decay, and ocean interaction. J. Appl. Meteor., 13, 739-751.

Rosenthal, S. L., 1971: The response of a tropical cyclone model to variations in boundary layer parameters, initial conditions, lateral boundary conditions, and domain size. Mon Wea. Rev., 99, 767-777.

Sheets, R. C., 1969: Some mean hurricane soundings J. Appl. Meteor., 8 134-146.

Sundqvist, H., 1972: Mean tropical storm behavior in experiments related to modification attempts. Tellus, 24, 6-12.

Tisdale, C. F., and P. F. Clapp, 1963: Origin and paths of hurricanes and tropical storms related to certain physical parameters at the air-sea surface. J. Appl. Meteor., 2, 358-367.

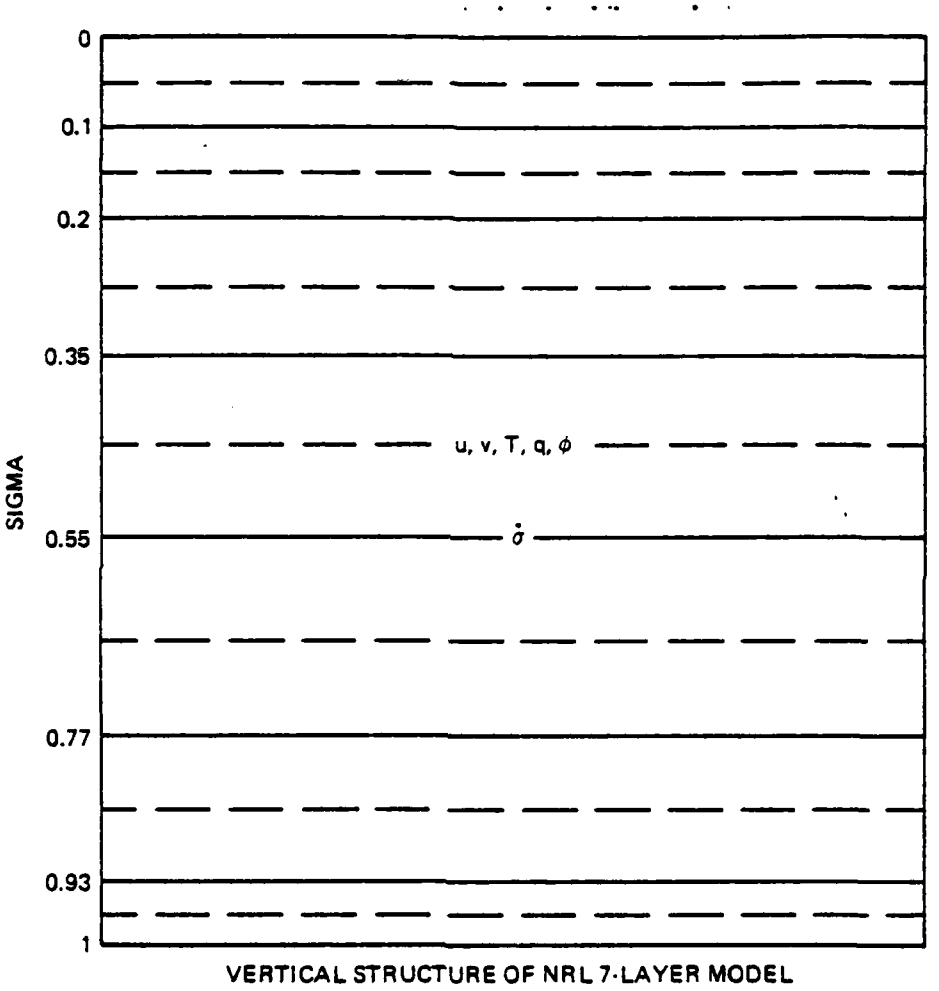

Fig. 1 — The vertical structure of the numerical model of the tropical cyclone

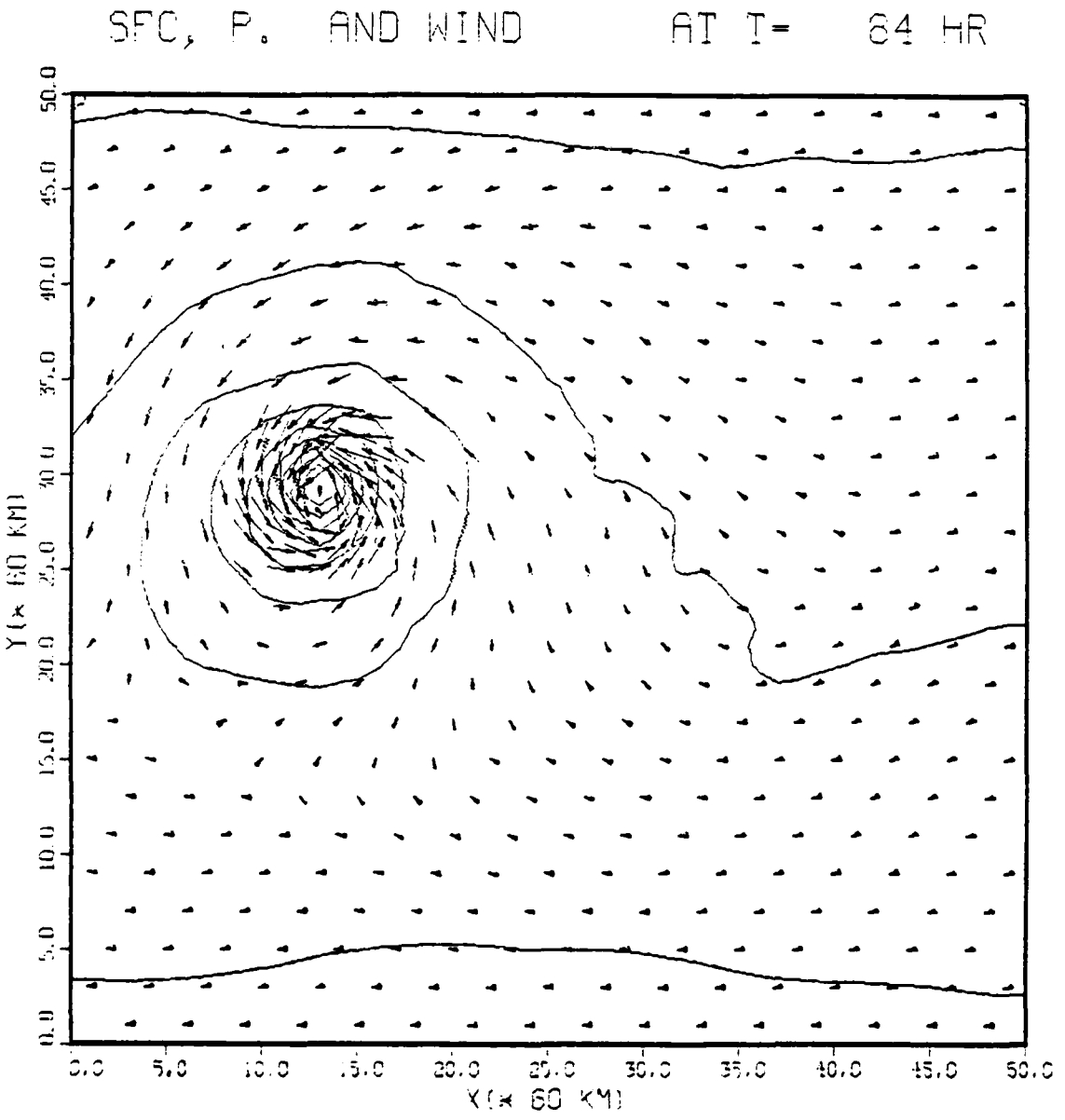

Fig. 2 — The boundary layer wind vector and surface pressure at 84 h of the control equipment (Exp. A)

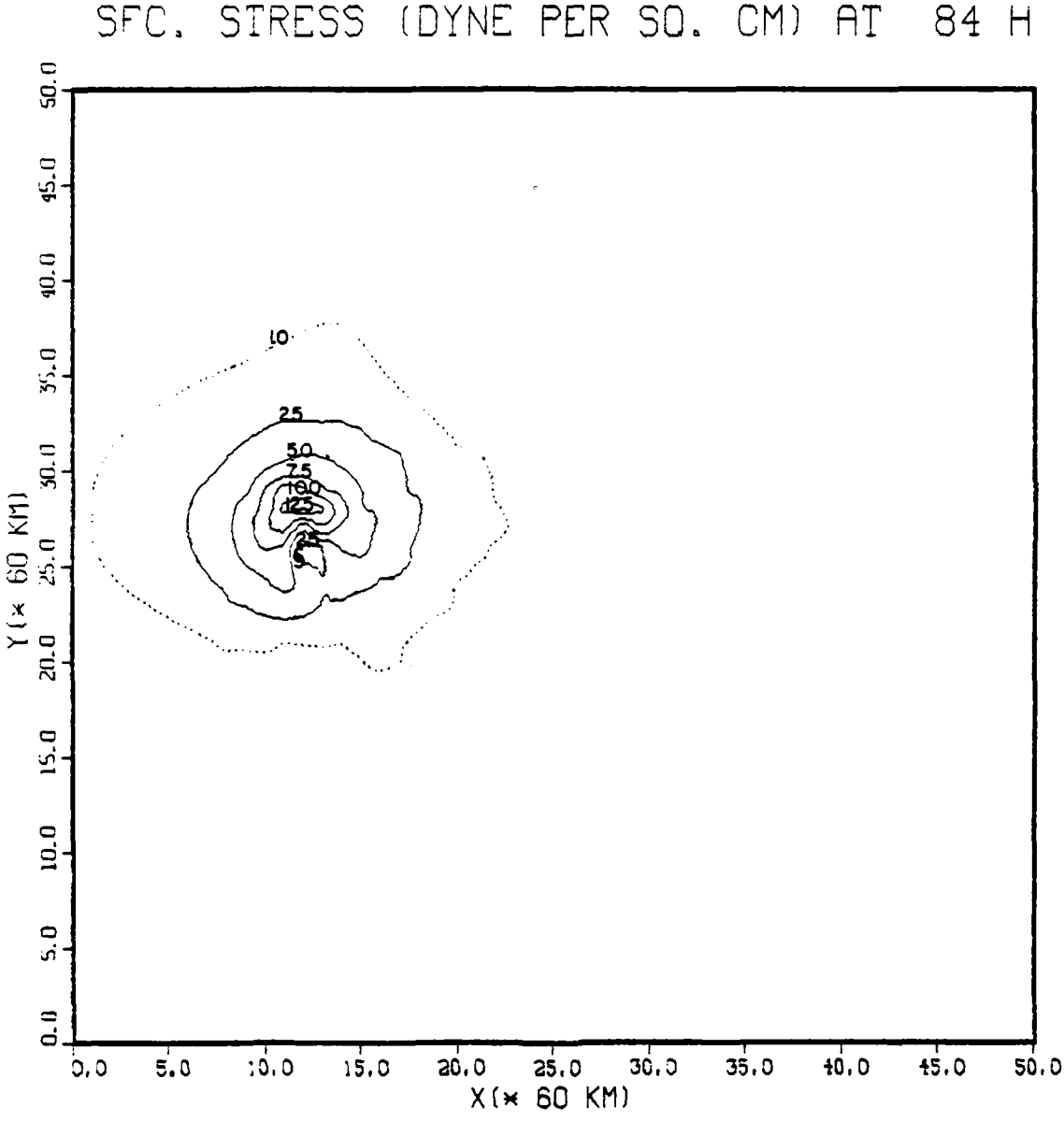

Fig. 3 — The surface stress (dyne cm^{-2}) at 84 h of Exp. A. Dotted line is 1 dyne cm^{-2} contour, solid lines are 2.5, 5.0, 7.5, ..., etc. dyne cm^{-2}.

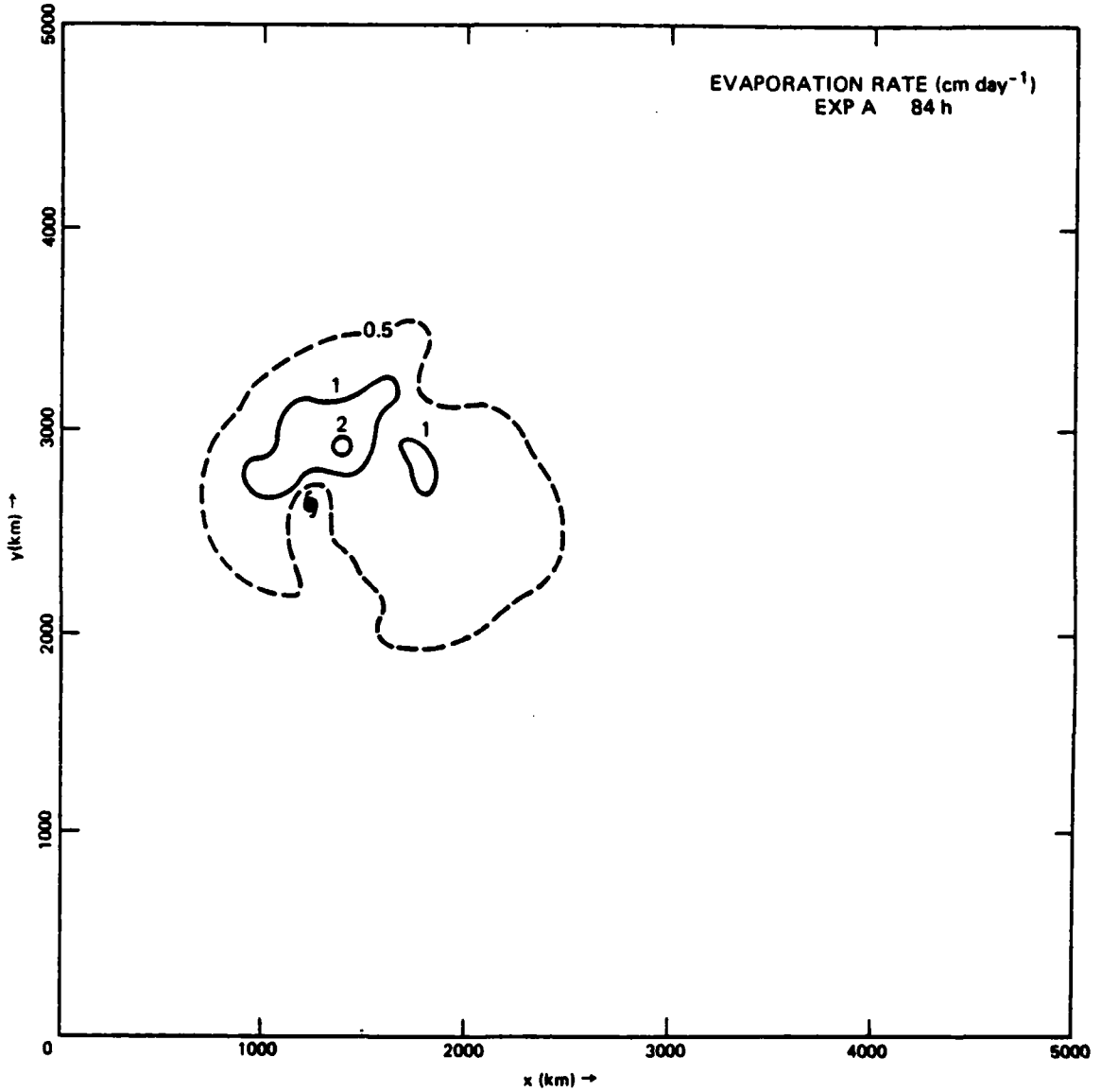

Fig. 4 — The evaporation rate (cm day^{-1}) at 84 h of Exp. A. Dotted lines are 0.5 cm day^{-1}, solid lines are 1, 2, ..., etc. cm day^{-1}.

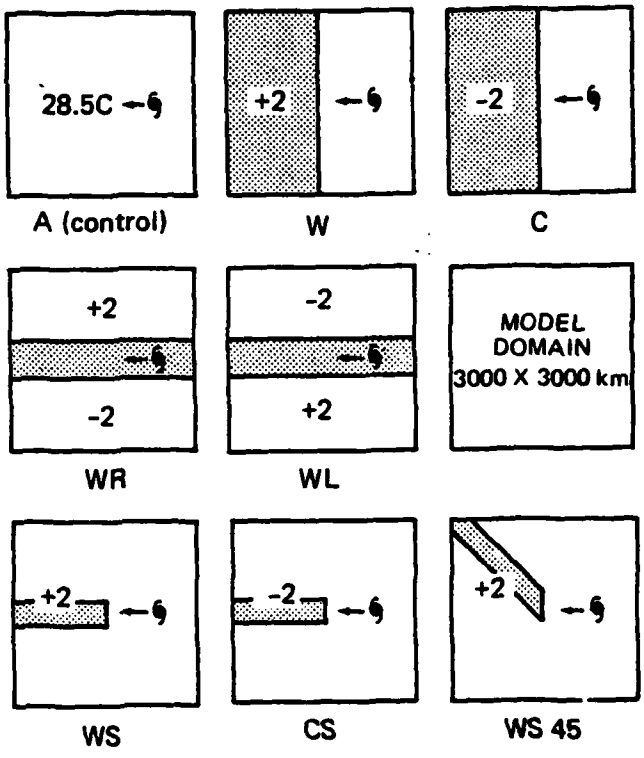

Fig. 5 — The various SST distributions tested

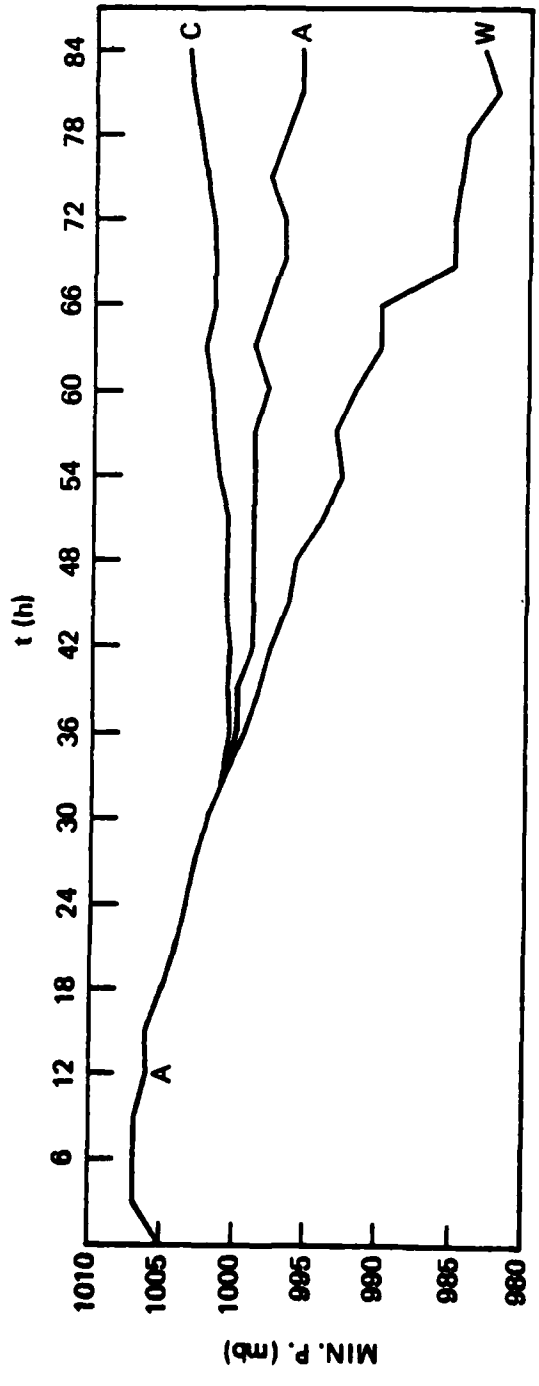

Fig. 6 — The time series of the minimum pressures of Exps. A, W, and C

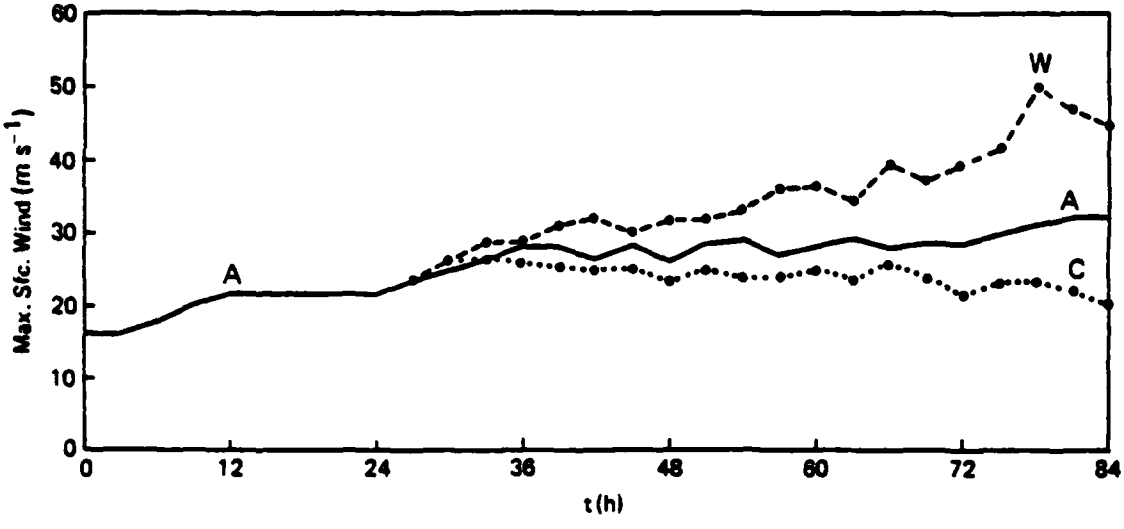

Fig. 7 — The time series of the maximum surface winds of Exps. A, W, and C

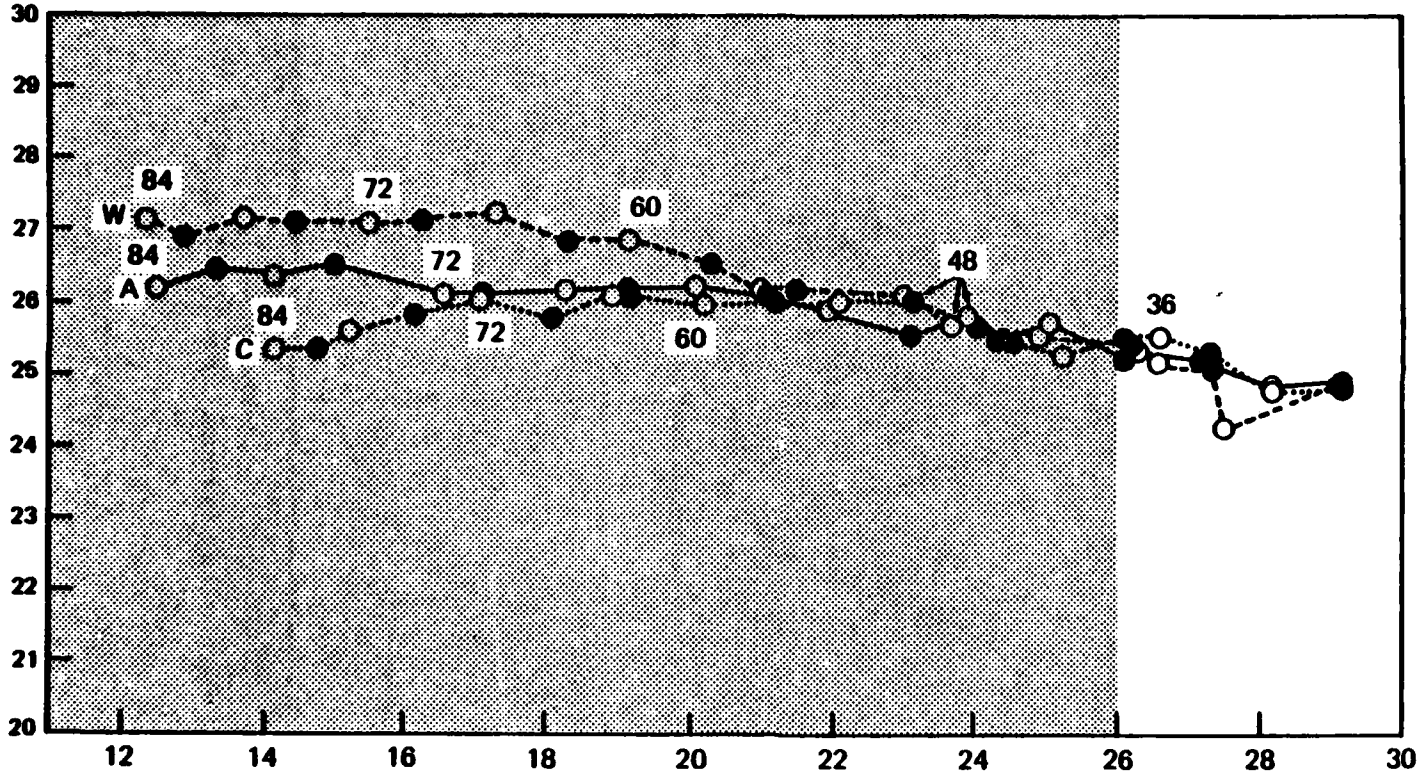

Fig. 8 — The paths of storm centers for Exps. A, W, and C. The numbers in curves denote times in an hour. The numbers on coordinates are grid points.

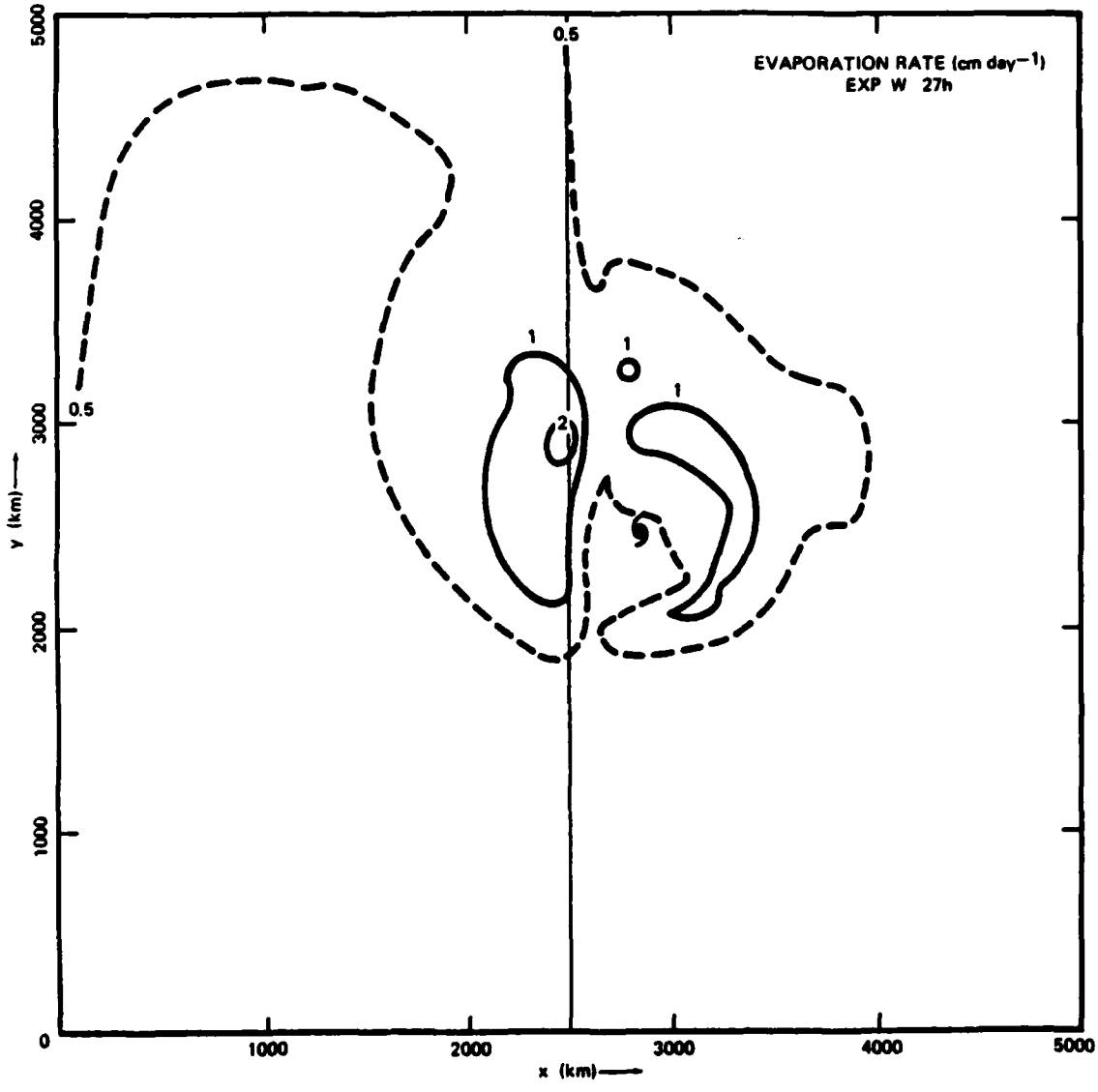

Fig. 9 — The evaporation rate at 27 h of Exp. W

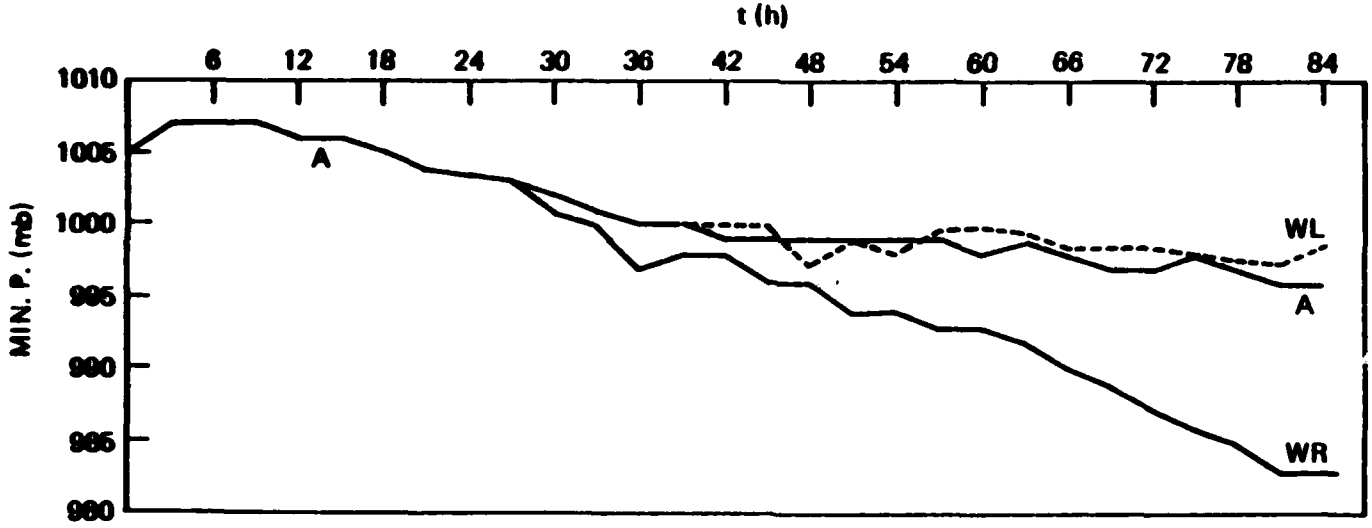

Fig. 10 — The time series of the minimum pressures of Exps. A, WR, and WL

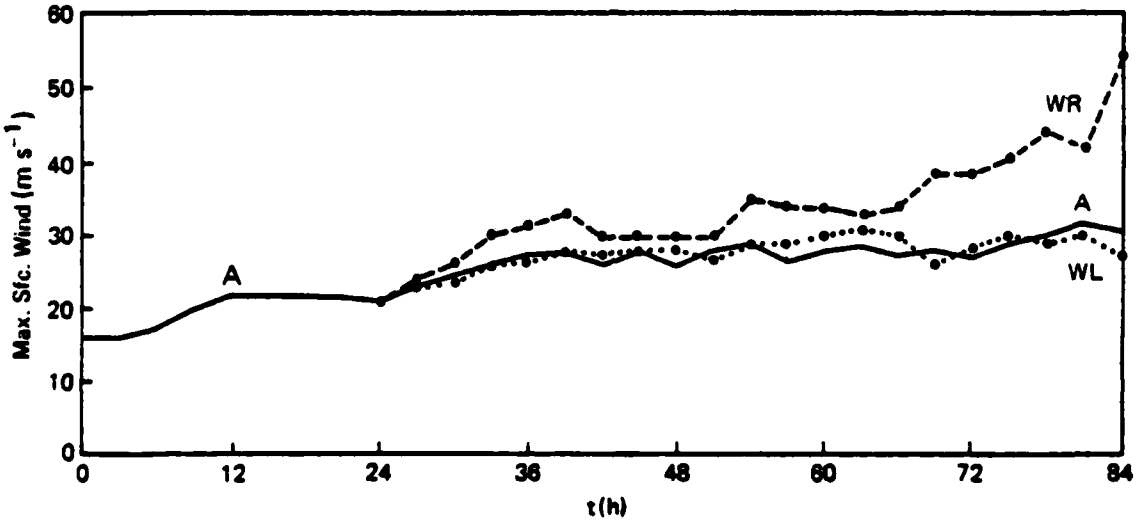

Fig. 11 — The time series of the maximum surface winds of Exps. A, WR, and WL

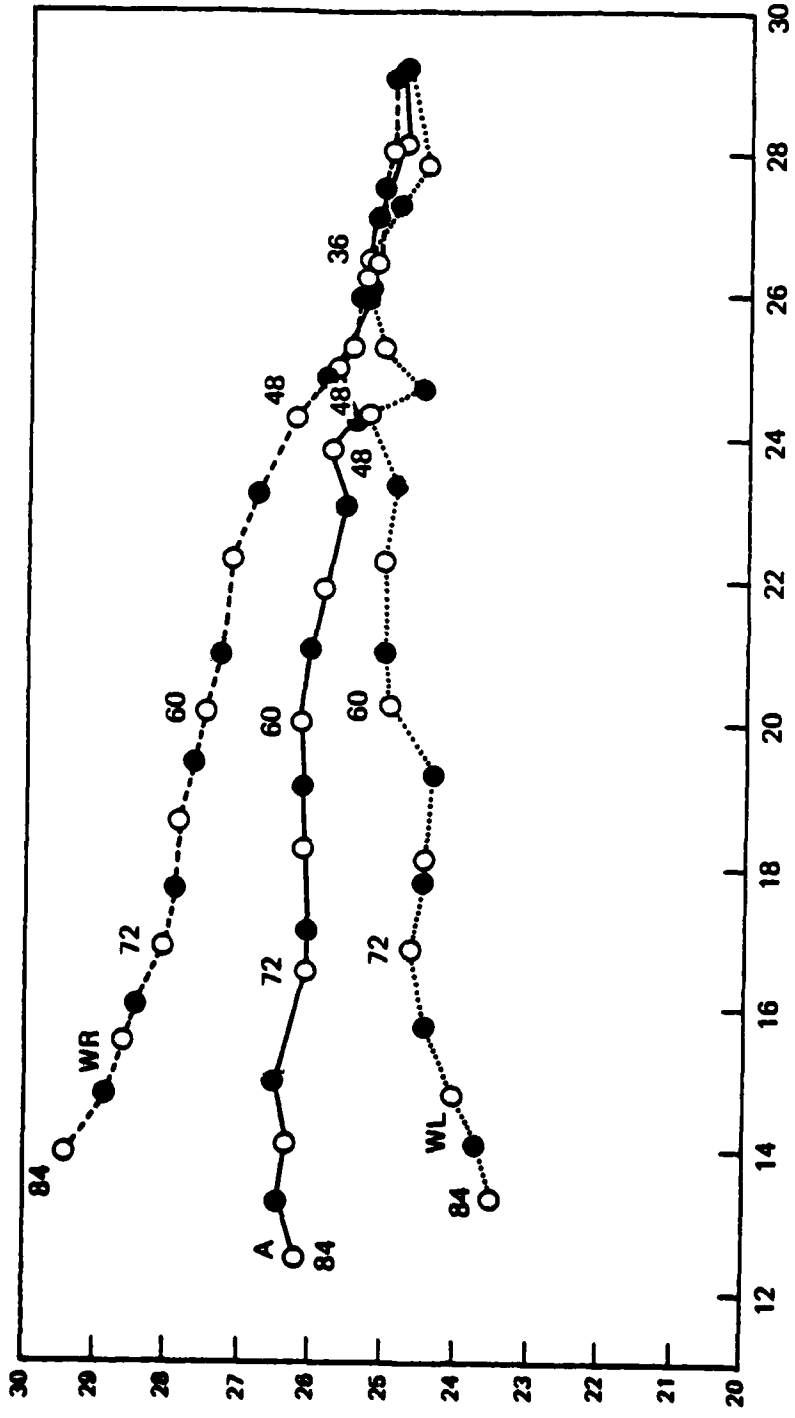

Fig. 12 — Same as Fig. 8, except for Exps. A, WR, and WL

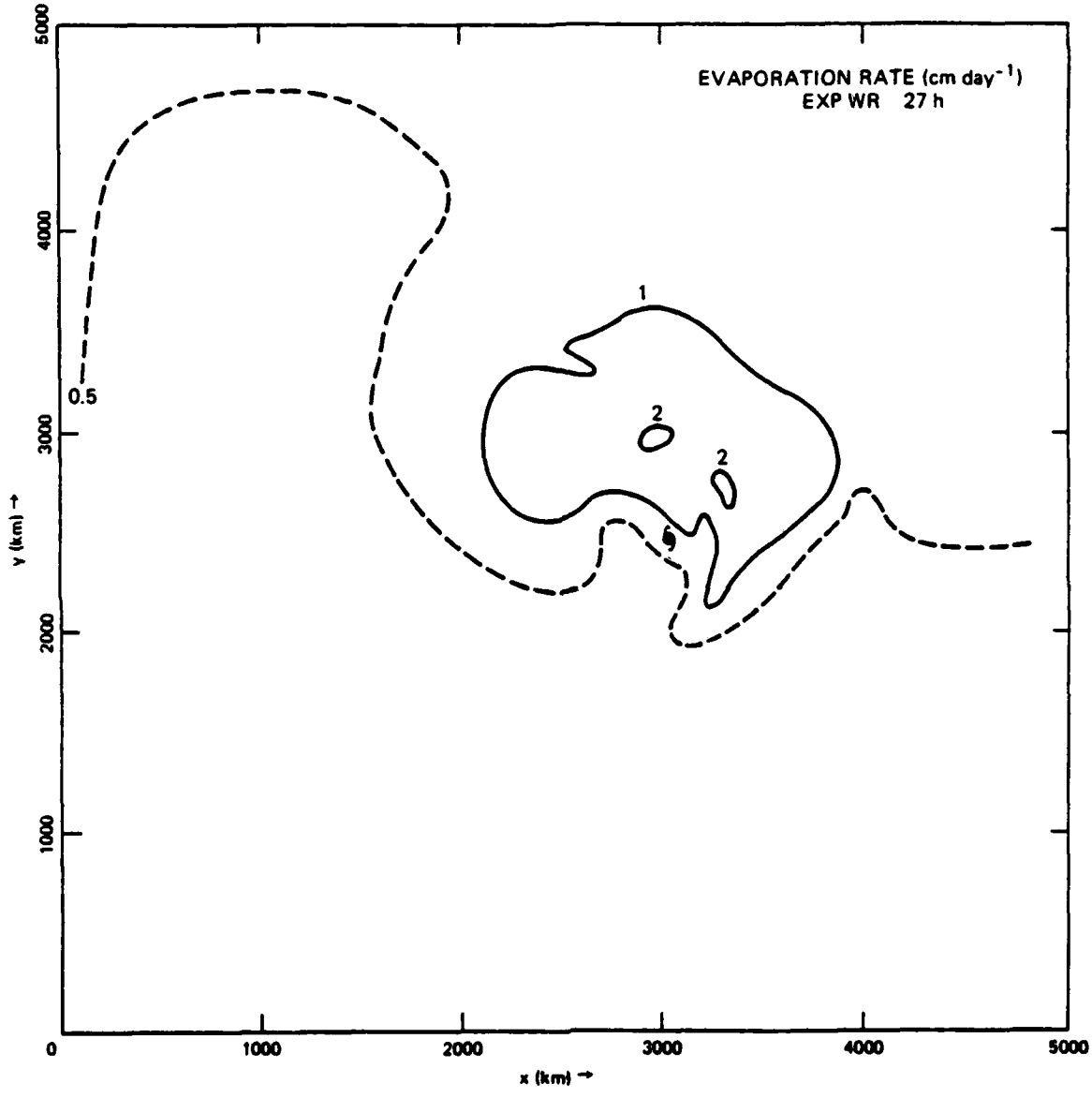

Fig. 13 — The evaporation rate (cm day^{-1}) at 27 h or Exp. WR

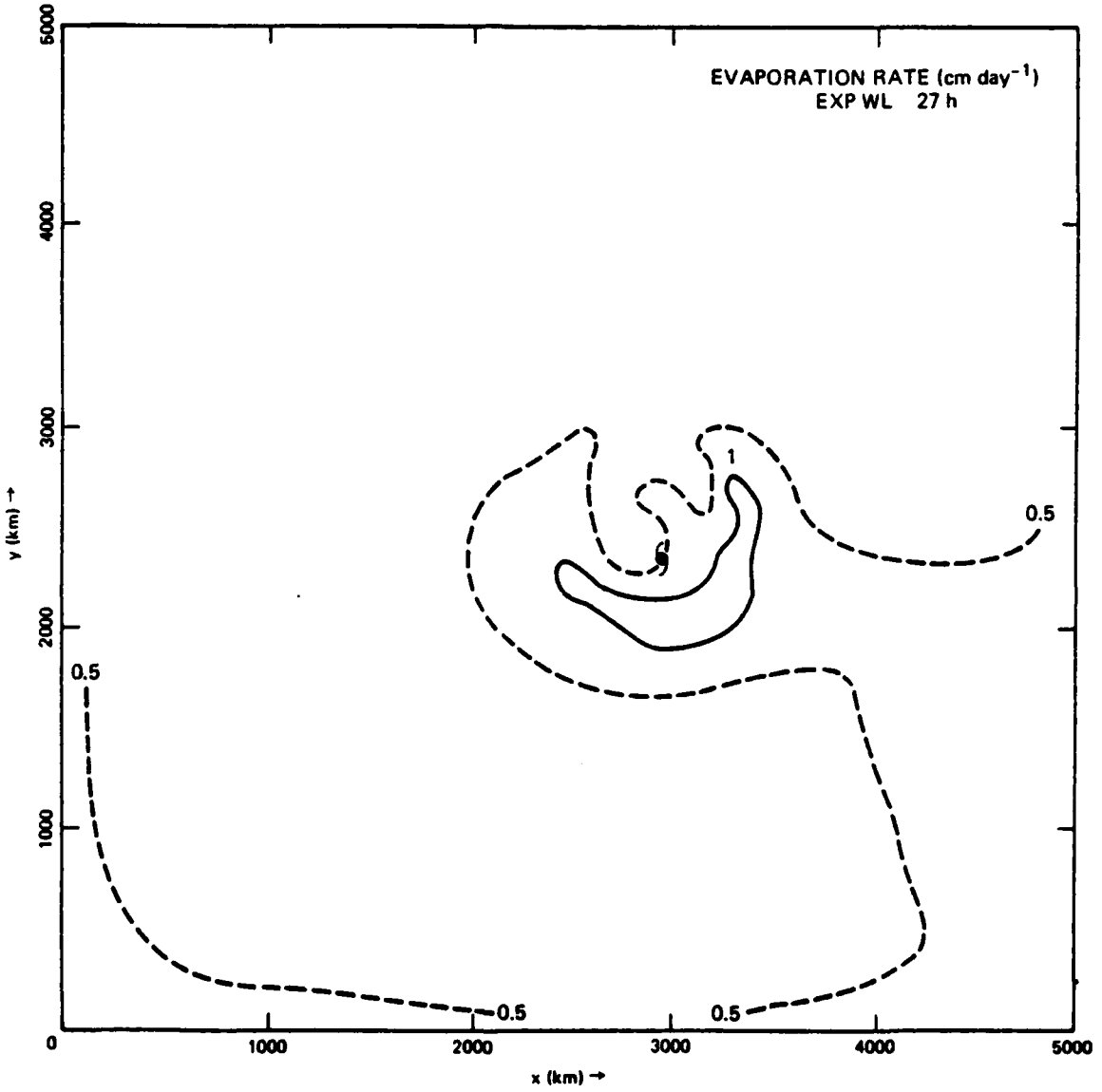

Fig. 14 — Same as Fig. 13 except for Exp. WL

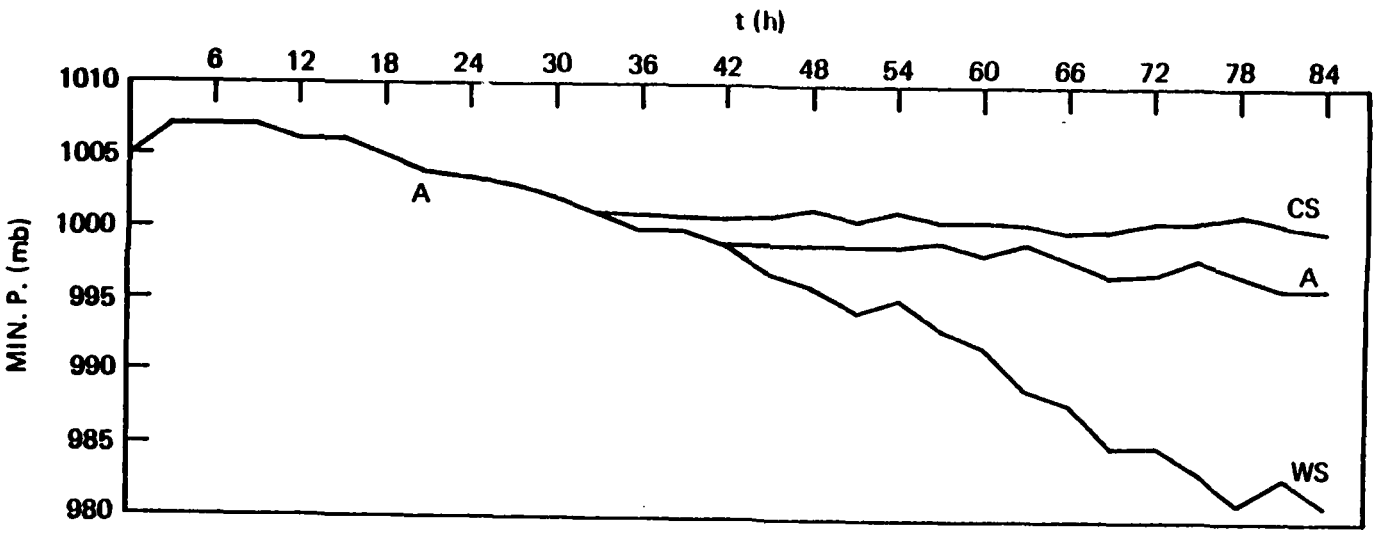

Fig. 15 — The time series of the minimum pressures of Exps. A, WS, and CS

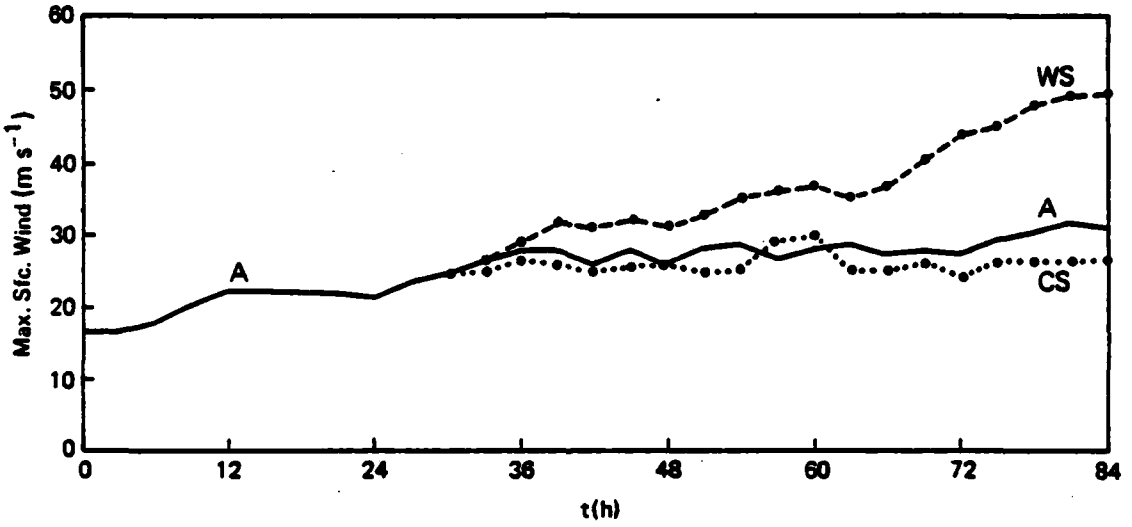

Fig. 16 — The time series of the maximum surface winds of Exps. A, WS, and CS

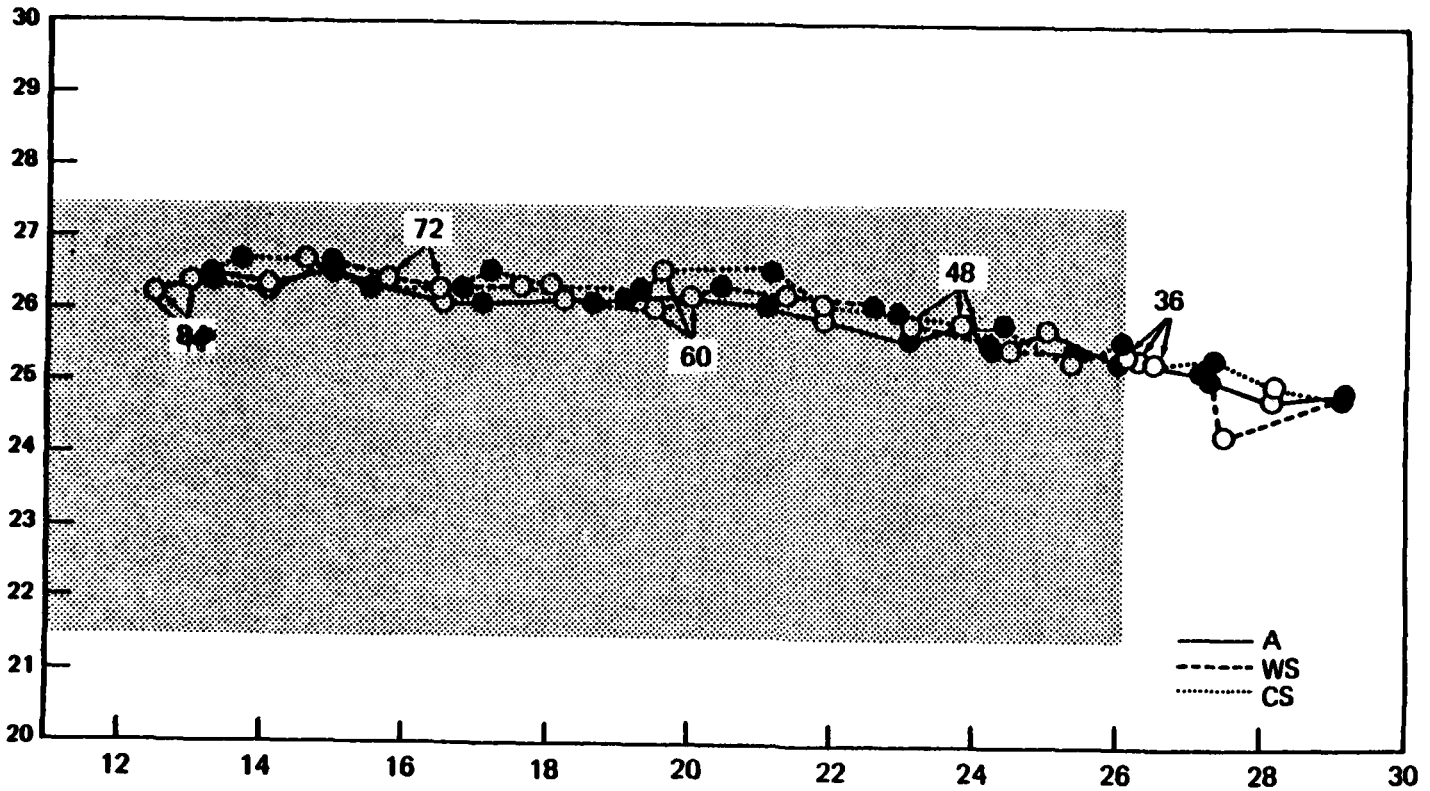

Fig. 17 — Same as Fig. 8 except for Exps. A, WS, and CS. The shaded area is the strip of warm or cold SST.

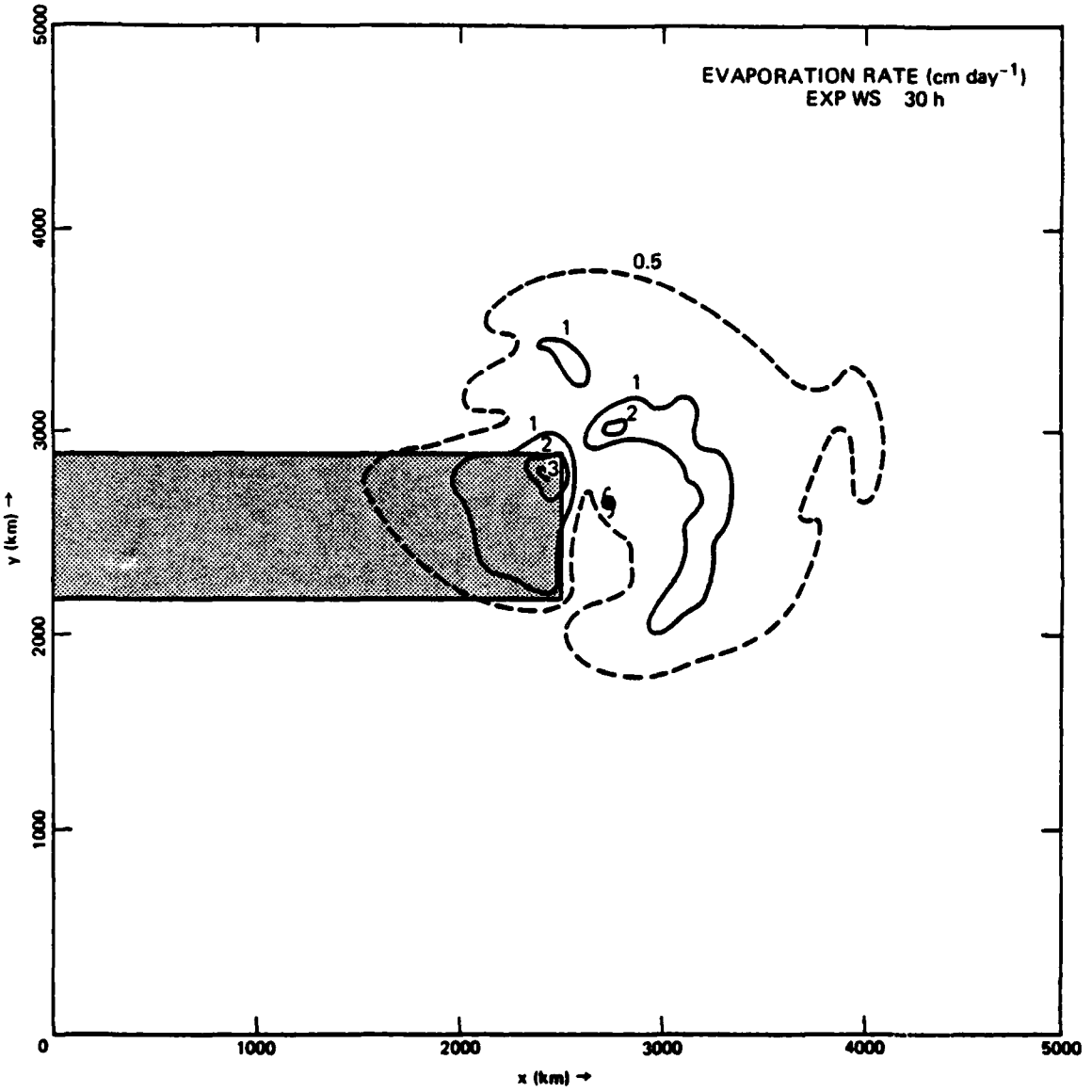

Fig. 18 — The evaporation rate (cm day^{-1}) at 30 h of Exp. WS. Shaded area is the warm strip.

DISTRIBUTION LIST

Chief of Naval Research
800 North Quincy Street
Arlington, VA 22217
ATTN: Code 465
Code 460

Chief of Naval Operations (OP-986G)
Navy Department
Washington, D.C. 20350

Chief of Naval Material (MAT-034)
Navy Department
Washington, D.C. 20360

Director
Naval Research Laboratory
Washington, D.C. 20375
ATTN: Code 4700, T. Coffey — 25 copies of open publication, 1 copy if otherwise
Code 4780, S. Ossakow — 150 copies if open publication, 1 copy if otherwise

Director
Office of Naval Research
Branch Office
495 Summer Street
Boston, Mass. 02210

Dr. Robert E. Stevenson
Office of Naval Research
Scripps Institution of Oceanography
LaJolla, CA 92037

Chairman
Naval Academy
Environmental Sciences Department
Annapolis, MD 21402

Dr. G. J. Haltiner
Department of Meteorology
Naval Postgraduate School
Monterey, CA 93940

Dr. Dale Leipper
Department of Oceanography
Naval Postgraduate School
Monterey, CA 93940

Naval Air Systems Command (AIR-370)
Washington, D. C. 20361

Naval Air Systems Command (AIR-OSF)
Washington, D.C. 20361

Naval Weapons Center
Code 602
China Lake, CA 93555

Naval Ocean Systems Center
Code 2220
San Diego, CA 92152

Commanding Officer
Naval Ocean R&D Act.
N.S.T.L. Station, MS 39529

Commanding Officer
Fleet Numerical Weather Central
Monterey, CA 93940

Commanding Officer
Naval Environment Prediction Research Facility
Monterey, CA 93940

Commander
Air Force Geophysics Laboratory
Bedford, MA 01730
ATTN: Dr. A. I. Weinstein

Commander
Air Weather Service
Scott AFB, ILL 52225
ATTN: LCOL R. Lininger

Office of the Chief of Research & Development
Department of the Army
Washington, D.C. 20301
ATTN: Environmental Sciences Division

Military Assistant
Environmental Sciences
OSD/ODDRE
Washington, D.C. 20301

Atmospheric Sciences Section
National Science Foundation
1800 G Street, N.W.
Washington, D.C. 20520

National Center for Atmospheric Research
Library Acquisitions
P. O. Box 1470
Boulder, CO 80302

Laboratory of Atmospheric Physics
Desert Research Institute
University of Nevada
Reno, Nevada 89507
ATTN: Dr. Patrick Squires

Carlspan Corporation
P. O. Box 235
Buffalo, NY 14221
ATTN: Mr. Roland Pilie

NORPAX
Scripps Institute of Oceanography
LaJolla, CA 92037
ATTN: Mr. Robert Peloquin

Geophysics Division
Pacific Missile Range
Pt. Mugu, CA 93042
ATTN: CDR. D. B. Pickenscher

Office of Naval Research
Pasadena Branch Office
1030 East Green Street
Pasadena, CA 91105
ATTN: Mr. Ben Cagle

Director
Naval Research Laboratory
Washington, D.C. 20375
ATTN: Code 8320

Defense Documentation Center — 12 copies
Cameron Street
Alexandria, VA 22314

Naval Research Laboratory — 20 copies
Washington, D.C. 20375
ATTN: Code 2628

END

DATE
FILMED

9-80

DTIC